Available online at www.sciencedirect.com
ScienceDirect
Remote Sensing of Environment 108 (2007) 163–170
Remote Sensing of Environment
www.elsevier.com/locate/rse

An improved algorithm for small and cool fire detection using MODIS data: A preliminary study in the southeastern United States

Wanting Wang [a,1], John J. Qu [a,b,*], Xianjun Hao [a,2], Yongqiang Liu [c,3], William T. Sommers [a,4]

[a] EastFIRE Lab, ESGS, College of Science, George Mason University, 4400 University Drive, Fairfax, VA 22030, USA
[b] NASA Goddard Space Flight Center (GSFC), Code 614.4, Greenbelt, MD 20771, USA
[c] USDA Forest Service, Forestry Sciences Laboratory, Athens, GA 30602, USA

Received 21 October 2005; received in revised form 18 October 2006; accepted 6 November 2006

Abstract

Traditional fire detection algorithms mainly rely on hot spot detection using thermal infrared (TIR) channels with fixed or contextual thresholds. Three solar reflectance channels (0.65 μm, 0.86 μm, and 2.1 μm) were recently adopted into the MODIS version 4 contextual algorithm to improve the active fire detection. In the southeastern United States, where most fires are small and relatively cool, the MODIS version 4 contextual algorithm can be adjusted and improved for more accurate regional fire detection. Based on the MODIS version 4 contextual algorithm and a smoke detection algorithm, an improved algorithm using four TIR channels and seven solar reflectance channels is described. This approach is presented with fire events in the southeastern United States. The study reveals that the T_{22} of most small, cool fires undetected by the MODIS version 4 contextual algorithm is lower than 310 K. The improved algorithm is more sensitive to small, cool fires in the southeast especially for fires detected at large scan angles.

Keywords: Algorithm; Remote Sensing; MODIS; Regional fire detection; Small, cool fires

1. Introduction

The southeastern United States is one of the areas in the country where wildland fires and prescribed fires are common (USDA Forest Service, 1998). An estimated 3.2 million hectares of wildland are burned per year in the southeastern United States (Wade et al., 2000). Most of the prescribed fires, and some of the wild fires, can be classified as understory surface fires, characterized by their small burn area and relatively low temperatures (Stanturf et al., 2002).

It is difficult to detect small and cool fires using current remote sensing algorithms because these fires do not emit sufficient radiation to penetrate dense canopies and cannot be easily distinguished from non-fire background radiation. To date, most algorithms are designed for global fire detection, and rely on identifying hot spots using thermal infrared (TIR) channels. The limitation of that technology is that false alarms are occasionally generated over certain surface types during the day time, and small, cool fires are oftentimes missed using relatively high thresholds optimized for global fire detection.

In this paper, we review problems with state of the art remote sensing of small, cool fires. We present an improved algorithm designed to detect small, cool fires in the southeastern United States with MODIS daytime observations. Two cases are presented to illustrate the performance of this algorithm.

2. Data and methods

2.1. Data and software

Reflectance from MODIS solar reflective channels in 1 km resolution, is employed to derive smoke pixels. The 0.41 μm

* Corresponding author. Department of Earth Systems and Geoinformation Sciences, George Mason University, 4400 University Drive, Fairfax, VA 22030, USA. Tel.: +1 7039933958.
E-mail address: jqu@scs.gmu.edu (J.J. Qu).
[1] Tel.: +1 7039941532.
[2] Tel.: +1 7039939322.
[3] Tel.: +1 7065594240.
[4] Tel.: +1 7039934012.

0034-4257/$ - see front matter © 2006 Elsevier Inc. All rights reserved.
doi:10.1016/j.rse.2006.11.009

and 0.94 μm channels, denoted by R_8 and R_{19}, respectively, are used to reject vegetation pixels. The 2.13 μm and 0.44 μm channels, denoted by R_7 and R_9, respectively, are applied to reject bare soil pixels. The reflectance from the blue channel is denoted by R_3, along with R_8 to reject water pixels.

Three thermal infrared channels and one solar reflective channel are applied to detect fire pixels. The brightness temperatures derived from 3.96 μm channels and the 11.03 μm channel are denoted by T_{22}, and T_{31}, respectively. The reflectance from the 0.86 μm channel in 1 km resolution is denoted by R_2. The reflectance from R_2, and the 0.65 μm channel, denoted by R_1 along with the brightness temperature derived for the 12.02 μm channel (T_{32}) and the 7.3 μm channel (T_{28}) are used to flag cloud pixels and reject cloud edge false alarms.

All data are downloaded from the Earth Observing System Data Gateway, Land Processes Distributed Active Archive Center (DAAC) (Justice et al., 2002b), including MODIS Level 1B Radiance product (MOD02/MYD02), geolocation data set (MOD03/MYD03), and thermal anomalies, fires, and biomass burning product (MOD14/MYD14).

To generate true color images, the MODIS Direct Readout (DR) software package MODISNDVI_DB_V2.1 is employed to calculate solar reflectance with atmospheric correction at three visible channels. The MODIS fire product at 18:50 GMT, December 20, 2004, not available at the DAAC, is generated by the DR software package MOD14-4. DR software, provided by the Direct Readout Laboratory at http://directreadout.gsfc.nasa.gov/. MATLAB is used to implement the improved algorithm.

2.2. Existing algorithms

A small number of authors (Dozier, 1981; Giglio et al., 1999; Langaas, 1993; Lasaponara et al., 2003) have focused on small fire detection based on theoretical analysis, fixed threshold method, or contextual algorithms using NOAA Advanced Very High Resolution Radiometer (AVHRR) multi-channel data. Since the Moderate Resolution Imaging Spectroradiometer (MODIS) instruments onboard Terra and Aqua began collecting data in February 2000 (Terra) and June 2002 (Aqua), satellite fire detection capability has been improved using two 3.96 μm channels.

In the MODIS version 3 active fire detection algorithm (Kaufman et al., 1998), sensitivity to relatively small fires were sacrificed in order to reduce persistent false alarms over certain surface types during the day time (Justice et al., 2002a). An enhanced contextual fire detection algorithm (Giglio et al., 2003) was recently used for MODIS version 4 fire products, in which the sensitivity to small, cool fires increased. This algorithm achieved significantly lower false alarm rates by using several solar reflectance channels to reject false alarms, and by adjusting the potential fire threshold and contextual thresholds in the earlier version of the MODIS contextual algorithm.

Contextual algorithms (e.g. Flasse & Ceccato, 1996; Giglio et al., 2003; Justice et al., 1996; Kaufman & Justice, 1998; Kaufman et al., 1998; Lee & Tag, 1990) use dynamic thresholds, relying on the contrast between a potential fire pixel and its background pixels (Boles & Verbyla, 2000) to detect fires. These algorithms are more flexible and effective in variable surface conditions than fixed threshold approaches (Flasse & Ceccato, 1996; Li et al., 2001). The MODIS contextual fire detection algorithm, designed for operational global fire monitoring, has the weakness for regional fire detection, including: fixed thresholds for identifying potential fire pixels; the assumption of a similar non-fire background nearby fire pixels; the effects of reflected solar radiation; the impact of undetected fires in the valid background pixels; problems caused by solar zenith angle and scan geometry; and the influence of atmospheric optical thickness. When applied to regional active fire detection in the southeast, small, cool fires are oftentimes missed due to special regional wildland fire patterns and environmental factors (Martin & Boyce, 1993; Stanturf et al., 2002). In addition, small, cool fires exhibit different characteristics depending on biome, amount of fuel burning, time of day, fire-line, season, geographic region, and view geometry (Giglio et al., 1999).

The MODIS contextual algorithm is composed of three basic parts, including preliminary thresholds to identify potential fire pixels, contextual tests to confirm fires among the potential fire pixels (Martin et al., 1999), and thresholds to reject false alarms. In the first part, the selection of fixed thresholds is subtle as an over-high setting runs a risk of omitting fire pixels. Meanwhile, an over-low setting causes more noise in deriving the parameters of the background pixels (Li et al., 2001) and generates more false alarms. The MODIS version 4 contextual algorithm employs fixed thresholds globally to identify potential fire pixels. For global applications, the preliminary thresholds cannot be set low enough to detect most small fires that can be physically detected for regional concern. Therefore, it needs improvement for fire monitoring and management at the regional scale.

Since fire severity varies with fuel type, fuel loading and weather conditions, potential fire thresholds should be contingent on these variables for regional applications (Li et al., 2001). Boles and Verbyla (2000) and Chuvieco and Martin (1994) demonstrated that fire detection accuracy was improved by using a fuel mask model. Csiszar et al. (2003) also suggest that adjusting thresholds to local conditions is necessary to reach a reasonable compromise between omission and commission errors for regional fire detection. These studies indicate that potential fire thresholds should be based on regional variations or they should be set as a function of a vegetation index for regional fire detection (Chuvieco & Martin, 1994; Martin et al., 1999).

In the second part of the MODIS algorithm, it is critical to determine valid neighboring pixels for every potential fire pixel, which will be used to derive the background parameters designed to set the remaining dynamic thresholds. The separation of fire pixels and non-fire background pixels becomes ambiguous with increasing background temperature caused by the presence of undetected background fires, seasonal change and certain surface types. This can directly affect the performance of the contextual algorithms. Giglio et al. (1999) excluded the eight pixels surrounding the potential fire pixel from the processing window in order to take out the fire contaminated background pixels. This algorithm showed a higher sensitivity to small, cool fires compared with the algorithms of Justice et al. (1996) and Flasse and Ceccato (1996).

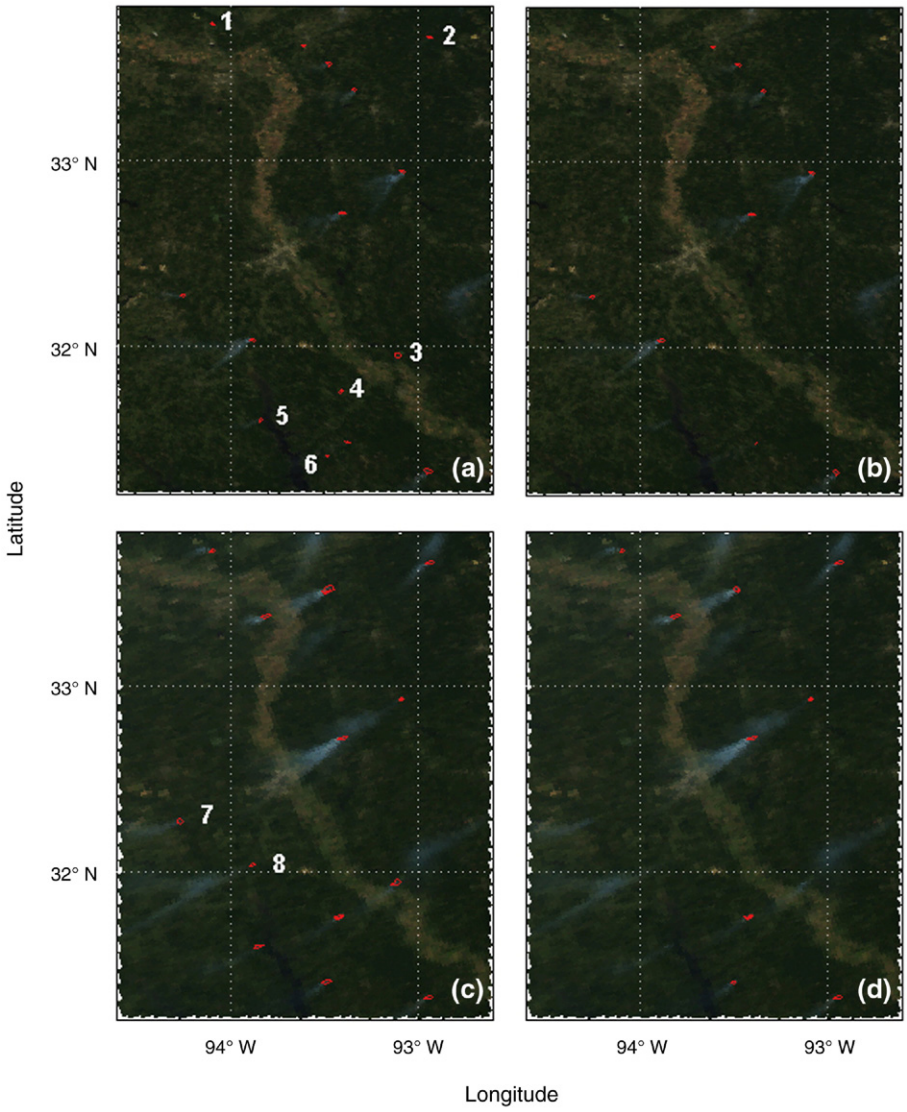

Fig. 1. Fire events detected by the MODIS contextual algorithm and the improved algorithm on September 29, 2003. Fire spots were marked in red with the background of MODIS 1 km true color images. Fire spots in Panels (a) and (c) were detected by the improved algorithm, and fire spots in Panels (b) and (d) were identified by the MODIS contextual algorithm. Panels (a) and (b) were observed at 17:15 GMT by MODIS/Terra, and Panels (c) and (d) were observed by MODIS/Aqua at 18:50 GMT.

The assumption that the surrounding non-fire pixels have similar brightness temperature is not appropriate in highly heterogeneous areas (Justice et al., 2002a). Reflected solar radiation around 4 μm channels causes high brightness temperature on bare soil, exposed rock, senescent or sparse vegetation, desert, tropical dry savanna and temperate grassland (summer). It is also the reason for sun glint effect over small bodies of water surface, coastline, wet soil and cirrus clouds, and misleading lower values on uneven forested areas (Csiszar et al., 2003; Giglio et al., 2003; Giglio et al., 1999; Lasaponara et al., 2003). The reflected solar radiation reduces the contrast between fire pixels and non-fire background pixels. Although the commission errors caused by reflected solar radiance have been decreased after the 3.75 μm band (AVHRR) was shifted to the 3.96 μm band in MODIS, the reflected solar radiation can only be reduced to the half of reflected sunlight at the 3.75 μm channel (Kaufman et al., 1998). In addition, increasing the solar zenith angle, or scan angle, or atmospheric optical thickness, also reduces the number of small, cool fires detected.

Due to the above reasons, contextual algorithms were adjusted by changing the thresholds for identifying potential fire pixels, tuning the type of background pixels and the size of the background window. This suggests the contextual algorithms are not self-adaptive enough for regional fire detection, and therefore regionally specified thresholds are necessary in order to develop effective regional fire detection algorithms (Lasaponara et al., 2003).

2.3. Overview of the improved algorithm

This regional fire detection algorithm is designed to reduce omission errors caused by fixed thresholds for identifying potential fire pixels. A new method based on identifying smoke

Table 1
Fire characters of fire events on September 29, 2003

Fire spots	Time (GMT)	T_{22} (K)	ΔT (K)	R_2	Scan angle (degree)
1	17:15#	309.0	16.2	0.171	19.5
	18:50	310.3	18.2	0.195	45.4
2	17:15#	308.1	15.9	0.156	26.5
	18:50	328.7	36.7	0.149	41.8
3	17:15#	320.0	25.5	0.157	28.6
	18:50#	323.9	28.8	0.157	44.4
4	17:15#	308.7	14.4	0.192	27.3
	18:50	315.2	21.5	0.182	45.6
5	17:15#	317.2	22.3	0.084	25.1
	18:50#	305.2	12.0	0.102	47.0
6	17:15#	309.4	16.0	0.161	27.5
	18:50	311.0	17.8	0.163	46.2
7	17:15	327.9	31.6	0.166	21.3
	18:50#	305.3	12.1	0.171	47.4
8	17:15	327.3	30.7	0.187	24.0
	18:50#	304.3	10.6	0.185	46.6

The fire spots with "#"can only be detected by the improved algorithm. The fire spots without "#" can be detected by both algorithms.

plumes (Xie et al., 2005) for obtaining potential fire areas was adopted to select potential fire pixels as the first stage of the algorithm. For the second part of the algorithm, the kernel of the enhanced contextual fire detection algorithm for MODIS (Giglio et al., 2003) is adopted for identifying fire pixels.

2.3.1. Cloud and water masking

A water mask is obtained from the MODIS geolocation data set (Justice et al., 2002b). The cloud detection approach adopts the technique used in the International Geosphere Biosphere Program (IGBP) AVHRR-derived Global Fire Product (Stroppiana et al., 2000) and the MODIS contextual algorithm (Giglio et al., 2003). The pixel that satisfies the following condition is considered as cloud:

$$(R_1 + R_2 > 0.9) \text{ or } (T_{32} < 265 \text{ K}) \text{ or } (R_1 + R_2 > 0.7 \text{ and } T_{32} < 285 \text{ K}) \quad (1)$$

The low potential fire threshold, which is used in the flowing step, introduces cloud edge false alarms. So, pixels with $T_{28} < 255$ K are rejected as cloud edge. Any pixels occupied by cloud or identified as water will not be processed.

2.3.2. Potential fire area

The cardinal feature of the MODIS contextual algorithm lies in the contextual tests, which are based on the identification of potential fire pixels with several fixed thresholds. One of the primary thresholds is $T_{22} > 310$ K. This criterion assumes any pixel with the $T_{22} < 310$ K is a non-fire pixel, but case studies of fire events in the southeast show T_{22} values of missed small, cool fires are lower than 310 K especially for observations at large scan angles. This assumption runs the high risk of omitting small, cool fires due to omitting potential fire pixels and including fire pixels into the valid background pixels.

The TIR radiance emitted by small, cool fires is partly blocked by high level canopies at the early stage of fire ignition or even the whole burning process. Most wildland fires and prescribed fires emit smoke due to the complex compositions of fuels and the percentage of fuel consumptions (Stanturf et al., 2002). Ward and Hardy (1991) indicated that emission factors for particles released from fires tend to increase inversely with combustion efficiency. In the southeast, fuel moisture is usually high, so the moisture released from fuels tends to absorb some of the heat energy from the fire. This limits combustion temperatures and fuel consumption percentages. Incomplete combustion usually produces more smoke emissions, so small, cool fires are more likely to have a longer smoldering combustion phase. The heat release rate from smoldering fires is usually not sufficient to lift the smoke into a well defined convective column. As a result, smoke plumes from small, cool fires stay near the ground in high concentrations (McMahon, 1983).

The first step of this improved algorithm is to identify smoke pixels among all the cloudless and non-water pixels using a smoke mask technique adopted from a smoke detection algorithm (Xie et al., 2005). The potential fire area around smoke pixels is calculated. Then, the pixels in the potential fire areas are examined by the attenuated potential fire thresholds based on the MODIS version 4 contextual algorithm. Those pixels satisfying the above conditions are identified as potential fire pixels and are further processed by the contextual tests.

The smoke detection algorithm developed by Xie et al. (2005) was adopted and modified for this study. Any cloudless and non-water pixels are considered as candidate smoke pixels. Then four criteria are applied to exclude vegetation pixels, bare soil pixels, and water pixels. These tests are:

$$0.5 \geq (R_8 - R_{19})/(R_8 + R_{19}) \geq 0.15 \quad (2)$$

$$(R_9 - R_7)/(R_9 + R_7) \geq 0.30 \quad (3)$$

$$(R_8 - R_3)/(R_8 + R_3) \leq 0.09 \quad (4)$$

$$R_8 \geq 0.09 \quad (5)$$

Those candidate pixels satisfying tests (2)–(5) are smoke pixels.

The range within which the smoke plumes can penetrate dense canopies indicates the distance between the fire spot and the observed smoke plume, denoted by the radius of potential fire area D. The regional climate data and biomass structure provide the parameters to derive the average maximum distance D_{max}. These parameters are minimum vertical wind speed V_{min}, average maximum surface wind speed S_{max}, and the maximum average height of the canopy layer H_{max}. Assuming the smoke plume disperses at a linear rate, D_{max} is derived by the relation $D_{max} = H_{max} * S_{max} / V_{min}$. Taking S_{max} as 9.0 ms^{-1} (Archer & Jacobson, 2003; Kaufman & Justice, 1998; Klink, 1999), H_{max} as 10 m, and V_{min} as 0.013 ms^{-1}, D_{max} is approximately 7 km. At the nadir view of MODIS, a 7 km radius' area is covered by a 14×14 pixel window. This area is defined as a potential fire area and is calculated for any smoke pixels to form a potential fire area mask. The horizontal wind profiles at the boundary layer are not distributed linearly, and the vertical wind shear and plume

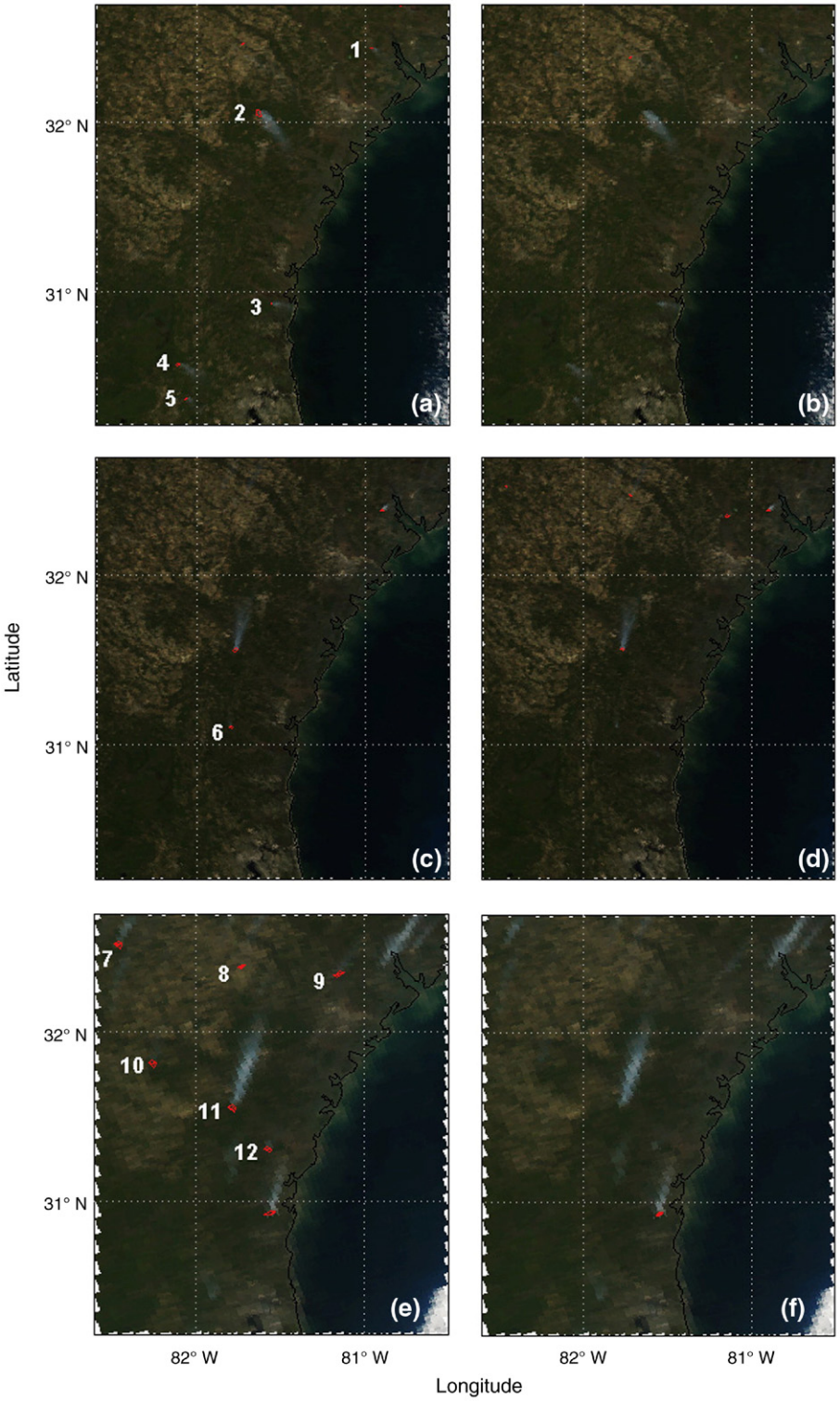

Fig. 2. Fire events detected by the MODIS contextual algorithm and the improved algorithm on December 20 and 21, 2004. Fire spots were marked in red with the background of MODIS 1 km true color image. Fire spots in Panels (a), (c), and (e) were detected by the improved algorithm, and fire spots in Panels (b), (d), and (f) were identified by the MODIS contextual algorithm. Panels (a) and (b), (c) and (d), (e) and (f) were observations on December 20, 18:50 GMT by MODIS/Aqua, December 21, 16:20 GMT by MODIS/Terra, and December 21, 17:55 GMT by MODIS/Aqua, in series.

buoyancy generated by fire lines or background atmospheric flow usually increase the dispersion speed of smoke plumes. Taking these factors into account, the actual radius is generally smaller than D_{max}.

2.3.3. Identification of potential fire pixels

Pixels within the potential fire area are considered as potential fire pixels if ($T_{22}>293$ K, $R_2<0.3$, and $\Delta T_{22}>10$ K), where $\Delta T_{22}=T_{22}-T_{31}$. These conditions are adopted from the

MODIS fire detection algorithm with a change in the T_{22} threshold, which is attenuated in order to increase the sensitivity to smaller, cooler fires. The T_{22} threshold is selected based on the statistical analysis of over 30 granules (800 fire pixels) dispersedly distributed in the southeast states in various seasons. The setting of 293 K for T_{22} threshold can reduce the omission errors caused by the corresponding threshold in the MODIS contextual algorithm, and decrease the number of fire pixels that are mistakenly included in the valid background pixels. The lower T_{22} threshold also reduces omission errors due to large scan angles, since the radiance of the object decreases at large scan angles and the lower threshold allows small, cool fire pixels at large scan angles to be further processed.

2.3.4. Contextual tests

Eight background parameters of valid background pixels are calculated for every potential fire pixel that has a qualified background window. These eight parameters are mean and mean absolute deviation of T_{22} ($\overline{T}_{22}$ and δ_{22}, respectively), mean and mean absolute deviation of T_{31} ($\overline{T}_{31}$ and δ_{31}, respectively), mean and mean absolute deviation of ΔT_{22} ($\Delta\overline{T}$ and $\delta_{\Delta T}$, respectively), mean absolute deviation of T_{22} for background fire pixels (δ'_{22}). The background pixels are in a background window centered on the potential fire pixel, and are defined as valid observations, which are not flagged as cloud, water, or potential fire pixels. The window starts from a 5×5 pixels and increases to a maximum of 21×21 pixels area, until at least 25% of the pixels within the window are background pixels. Those potential fire pixels, which fail to achieve a background window, are classified as unknown pixels and are not subjected to further testing. However, if the T_{22} values of the pixels are greater than 360 K, the pixels are classified as fire pixels.

The following contextual tests are adopted from the MODIS contextual tests. These tests are:

$$\Delta T > \Delta\overline{T} + 3.5\delta_{\Delta T} \tag{6}$$

$$\Delta T > \Delta\overline{T} + 6\ \mathrm{K} \tag{7}$$

$$T_{22} > \overline{T}22 + 3\delta_{22} \tag{8}$$

$$T_{31} > \overline{T}31 + \delta_{31} - 4\ \mathrm{K} \tag{9}$$

$$\delta'_{22} > 5\ \mathrm{K} \tag{10}$$

Potential fire pixels that satisfy the following conditions are identified as fire pixels: {$T_{21}>360$ K} or {tests (6)–(8) are true and [test (9) or test (10) is true]}.

2.3.5. Case study

Two wildland fire cases detected by both MODIS/Terra and MODIS/Aqua in the hot season and the cold season are selected to present the performance of the improved algorithm. One case is fire events on December 20–21, 2004 at the border region between Georgia and Florida along the Atlantic coast, and the border region between Mississippi and Alabama along the Gulf coast. The second fire event occurred on September 29, 2003, located in the Red River Basin in Mississippi.

Table 2
Fire characters of fire events on December 20 and December 21, 2004

Fire spots	Time (GMT)	T_{22} (K)	ΔT (K)	R_2	Scan angle (degree)
1	Dec. 20, 18:50#	296.4	17.8	0.108	29.2
	Dec. 21, 16:20	329.4	43.3	0.115	17.8
2	Dec. 20, 18:50#	302.8	23.1	0.105	24.2
3	Dec. 20, 18:50#	293.0	13.2	0.123	23.1
	Dec. 21, 17:55	313.3	26.7	0.141	51.4
4	Dec. 20, 18:50#	300.9	19.9	0.137	19.0
5	Dec. 20, 18:50#	296.8	16.1	0.124	18.9
6	Dec. 21, 16:20#	302.2	16.4	0.107	14.3
7	Dec. 21, 17:55#	297.7	11.7	0.118	52.0
8	Dec. 21, 17:55#	301.8	14.2	0.125	50.6
9	Dec. 21, 17:55#	300.9	15.6	0.090	49.3
10	Dec. 21, 17:55#	305.3	18.7	0.131	52.2
11	Dec. 21, 16:20	315.2	26.7	0.110	13.5
	Dec. 21, 17:55#	306.1	18.4	0.132	51.4
12	Dec. 21, 17:55#	298.9	11.7	0.120	51.2

The fire spots with "#"can only be detected by the improved algorithm. The fire spots without "#" can be detected by both algorithms.

Each case is calculated using both the improved algorithm and the MODIS contextual algorithm. Fire events detected by the MODIS contextual algorithm are considered true fires, since the MODIS contextual algorithm has been validated systematically and offers a significantly lower false alarm rate. Comparative analysis is conducted between earlier and later observations of fire events which are undetectable using the MODIS contextual algorithm but detectable using the improved algorithm. If a previously undetected fire event is subsequently detected using the MODIS contextual algorithm, and/or the improved algorithm, and the event is accompanied by obvious smoke plumes, this fire event is believed to be a true fire event which was previously omitted by the MODIS contextual algorithm. Fire events, which are only detectable using the improved algorithm at earlier time, but not detectable by both algorithms in subsequent observations, are considered uncertain spots. Uncertain spots are further inspected using MODIS 250 m true color images. In all cases investigated MODIS 250 m true color images of the corresponding regions showed that the uncertain spots were accompanied by obvious smoke plumes. This supports the supposition that they are indeed fire spots.

3. Results and concluding remarks

Among the fire events in the Red River Basin (Fig. 1), eight fire spots undetected by the MODIS contextual algorithm are numbered in Panel (a) and (c). Taking fire spot 2 as an example, the improved algorithm detected this thermal anomaly at 17:15 GMT (Panel a), and both algorithms identified this spot as an active fire with an obvious smoke plume at 18:50 GMT (Panel c and d). In Table 1, both T_{22} and ΔT for fire spot 2 increased by approximately 20 K during a period of 1.5 h. This proves that the fire at 17:15 GMT was an active fire. Fire spot 3 at 17:15

GMT and 18:50 GMT, and fire spot 5 at 17:15 GMT satisfy the threshold of T_{22} >310 K (Table 1) and contextual thresholds, but they are not identified by the MODIS contextual algorithm. This indicates that the false alarm rejection thresholds in the MODIS contextual algorithm cause omission errors.

In Fig. 2, fire spots 1 to 12, marked in Panel (a), (c) and (e), are omitted by the MODIS contextual algorithm. Although fire spots 1, 5 and 6 are not accompanied by obvious smoke plumes in the 1 km resolution MODIS true color images, corresponding MODIS 250 m true color images show that all of these three spots are indeed accompanied by smoke plumes. Spots 7 to 12 are fire spots because they are accompanied by obvious smoke plumes even in the 1 km images. Three spots in Panel (d) are detected as fire spots by the MODIS contextual algorithm. The left and the right spots are not accompanied by smoke plumes even in the MODIS 250 m true color image. The spot in the middle is accompanied by unobvious smoke in the MODIS 250 m true color image. This case presents a limitation of the improved algorithm and indicates that fire spots lacking a detectable smoke plume in a 1 km resolution image will be omitted.

Figs. 1(c) and 2(e) show that the improved algorithm is more sensitive to small, cool fires, especially for observations at large scan angles (Tables 1 and 2). In the two fire events on September 29, 2003 and December 20–21, 2004, there are a total of 22 fire spots which are omitted by the MODIS contextual algorithm, but detected by the improved algorithm. The improved algorithm fails to detect small fires lacking a visible smoke plume unless they are within the potential fire area of other fires.

The characteristics of small, cool fires undetected by the MODIS contextual algorithm are listed in Tables 1 and 2. The T_{22} brightness temperatures of these small, cool fires are lower than 310 K, a critical threshold for identifying potential fire pixels in the MODIS contextual algorithm. The thresholds of ΔT and R_2 in the MODIS contextual algorithm are valid for small, cool fires undetected by the MODIS contextual algorithm. The fire characteristics of small, cool fires suggest that the threshold of T_{22} greater than 310 K is too high to detect small, cool fires in the southeast, and the corresponding adjustment in the improved algorithm is reasonable. The improved algorithm is less sensitive to negative effects caused by large view angles mainly due to decreasing the T_{22} threshold to 293 K.

Acknowledgements

We would like to thank Yong Xie for his assistance with the smoke detection algorithm. We appreciate the anonymous reviewers for their constructive comments and suggestions. This study was funded by the USDA Forest Service, Southern Research Station SRS 04-CA-11330136-170.

References

Archer, C. L., & Jacobson, M. Z. (2003). Spatial and temporal distributions of U.S. winds and wind power at 80 m derived from measurements. *Journal of Geophysical Research*, *108*, 4289–4309.

Boles, S. H., & Verbyla, D. L. (2000). Comparison of three AVHRR-based fire detection algorithms for interior Alaska. *Remote Sensing of Environment*, *72*, 1–16.

Chuvieco, E., & Martin, M. P. (1994). A simple method for fire growth monitoring using AVHRR channel 3 data. *International Journal of Remote Sensing*, *15*, 3141–3146.

Csiszar, I., Abdelgadir, A., Li, Z., Jin, J., Fraser, R., & Hao, W. M. (2003). Interannual changes of active fire detectability in North America from long-term records of the Advanced Very High Resolution Radiometer. *Journal of Geophysical Research*, *108*(D2), 4075–4085.

Dozier, J. (1981). A method for satellite identification of surface temperature fields of subpixel resolution. *Remote Sensing of Environment*, *11*, 221–229.

Flasse, S. P., & Ceccato, P. (1996). A contextual algorithm for AVHRR fire detection. *International Journal of Remote Sensing*, *17*, 419–424.

Giglio, L., Kendall, J. D., & Justice, C. O. (1999). Evaluation of global fire detection using simulated AVHRR infrared data. *International Journal of Remote Sensing*, *20*, 1947–1985.

Giglio, L., Descloitres, J., Justice, C. O., & Kaufman, Y. J. (2003). An enhanced contextual fire detection algorithm for MODIS. *Remote Sensing of Environment*, *87*, 273–282.

Justice, C. O., Giglio, L., Korontzi, S., Owens, J., Morisette, J. T., Roy, D., et al. (2002a). The MODIS fire products. *Remote Sensing of Environment*, *83*, 244–262.

Justice, C. O., Kendall, J. D., Dowty, P. R., & Scholes, R. J. (1996). Satellite remote sensing of fires during the SAFARI campaign using NOAA advanced very high resolution radiometer data. *Journal of Geophysical Research*, *101*, 23851–23863.

Justice, C. O., Townshend, J. R. G., Vermote, E. F., Masuoka, E., Wolfe, R. E., Saleous, N., et al. (2002b). An overview of MODIS Land data processing and product status. *Remote Sensing of Environment*, *83*, 3–15 (http://edcimswww.cr.usgs.gov/pub/imswelcome/).

Kaufman, Y., & Justice, C. O. (1998). MODIS fire products algorithm technical background document. URL: http://modis.gsfc.nasa.gov/data/atbd/atbd_mod14.pdf. pp29.

Kaufman, Y., Justice, C. O., Flynn, L. P., Kendall, J. D., Prins, E. M., Giglio, L., et al. (1998). Potential global fire monitoring from EOS-MODIS. *Journal of Geophysical Research*, *103*, 215–238.

Klink, K. (1999). Trends in mean monthly maximum and minimum surface wind speeds in the coterminous United States, 1961 to 1990. *Climate Research*, *13*, 193–205.

Langaas, S. (1993). A parameterised bispectral model for savanna fire detection using AVHRR night images. *International Journal of Remote Sensing*, *14*, 2245–2262.

Lasaponara, R., Cuomo, V., Macchiato, M. F., & Simoniello, T. (2003). A self-adaptive algorithm based on AVHRR multitemporal data analysis for small active fire detection. *International Journal of Remote Sensing*, *24*, 1723–1749.

Lee, T. M., & Tag, P. M. (1990). Improved detection of hotspots using the AVHRR 3.7 μm channel. *Bulletin of the American Meteorological Society*, *71*, 1722–1730.

Li, Z., Kaufman, Y. J., Ichoku, C., Fraser, R., Trishchenko, A., Giglio, L., et al. (2001). A review of satellite fire detection algorithms: principles, limitations and recommendations. In F. Ahern, J. Goldammer, & C.O. Justice (Eds.), *Global and regional fire monitoring from space: Planning a coordinated international effort* (pp. 199–226). The Hague: SPB Academic.

Martin, W. H., & Boyce, S. G. (1993). Introduction: the southern setting. In William H. Martin, Stephen G. Boyce, & Arthur C. Echternacht (Eds.), *Biodiversity of the Southeastern United States upland terrestrial communities* (pp. 1–46). New York: John Wiley.

Martin, P., Ceccato, P., Flasse, S., & Downey, I. (1999). Fire detection and fire growth monitoring using satellite data. In E. Chuvieco (Ed.), *Remote sensing of large wildfires in the European Mediterranean Basin* (pp. 212). Berlin/Heidelberg: Springer-Verlag.

McMahon, C. K. (1983). Characteristics of forest fuels, fires and emissions. *The 76th annual meeting of the air pollution control association. Atlanta, Georgia, June 19–24.* http://www.treesearch.fs.fed.us/pubs/1015

Stanturf, J. A., Wade, D. D., Waldrop, T. A., Kennard, D. K., & Achtemeier, G. L. (2002). Fire in Southern Forest Landscape, in Southern forest resource assessment. In David N. Wear & John G. Greis (Eds.), *Gen. Tech. Rep. SRS-*

53 (pp. 635). Asheville, NC: U.S. Department of Agriculture, Forest Service, Southern Research Station.

Stroppiana, D., Pinnock, S., & Gregoire, J. -M. (2000). The global fire product: daily fire occurrence from April 1992 to December 1993 derived from NOAA AVHRR data. *International Journal of Remote Sensing*, *21*, 1279−1288.

USDA Forest Service (1998). *1991–1997 wildland fire statistics* (pp. 141). US Dep Agric, For Serv, Fire and Aviation Management.

Wade, D. D., Brock, B. L., Brose, P. H., Grace, J. B., Hoch, G. A., & Patterson III, W. A. (2000). Fire in eastern ecosystems, in Wildland fire in ecosystems: effects of fire on flora. In J. K. Brown & J.K. Smith (Eds.), *Gen. Tech. Rep. RMRS-42* (pp. 53−96). Ogden, UT: U.S. Department of Agriculture, Forest Service, Rocky Mountain Research Station.

Ward, E. D., & Hardy, C. C. (1991). Smoke emissions from wildland fires. *Environment International*, *17*, 117−134.

Xie, Y., Qu, J., Hao, X., Xiong, J., & Che, N. (2005). Smoke plume detecting using MODIS measurements in eastern United States. *EastFIRE Conference Proceedings, Fairfax, VA, May 11–13*.